CHAPTER 5

EFFECT OF PRE HOT CORROSION ON HIGH CYCLE FATIGUE BEHAVIOR OF SUPERALLOY IN718 AT 600°C

5.1 INTRODUCTION

The Ni-Fe based superalloy IN718 is mostly used as disc and blade material in compressor section of the advanced power plants and aero engines **[Sunderaraman et al. (1988)]**. Gas turbines operating in the marine environment, suffer from hot corrosion **[Collier et al. (1988), Lai (2007)]**. It is well known that in hot corrosion, salt/salt mixtures fuse and accelerate the rate of oxidation and sulfidation of superalloys. It is evident from the literature that little attention has been paid on high cycle fatigue properties of the superalloy IN718 in the simulated marine environment. The present investigation was undertaken to examine the effect of pre-hot corrosion at 600ºC for 100 h in the salt mixture of $75Na_2SO_4 + 15NaCl + 10V_2O_5$ (wt.%) on high cycle fatigue behavior of the superalloy IN718 at 600ºC.

Fatigue samples were cleaned with acetone, weighed, and preheated to temperature of 150 – 200°C by holding the sample horizontally at a height of ~ 30 mm above the hot plate and rotating at 5 rpm. Salt spraying was carried out in middle section of the hour glass sample. Salt deposit of 3.5 - 4 mg/cm^2 was found to form a uniform and intact salt layer on the HCF specimen. Salt coated HCF specimens were subjected to high cycle fatigue test at the frequency of 30 Hz. It was observed that the salt layer peeled off soon

after the start of the fatigue test, therefore, the salt coated samples were hot corroded at 600ºC for 100 h before the HCF test at 600ºC in the air. The hot corroded samples were kept in an oven at 150ºC to avoid absorption of moisture from air. Fully reversed ($R = -1$) HCF tests were carried out in air under stress control mode on both the as heat treated and pre hot corroded specimens. Tests were carried out at 600 °C, at different stress amplitudes of ±450 MPa, ±500 MPa, ±550 MPa, ±600 MPa, ±650 MPa, ±700 MPa and ±750 MPa at a constant frequency of 30 Hz.

5.2 RESULTS

5.2.1 MICROSCOPIC CHARACTERIZATION

Digital photograph of the salt coated and pre hot corroded specimen at 600 °C for 100 h, prior to HCF testing is shown in Fig. 5.1. The specimen surface was found severely corroded but intact after exposure in the air at 600ºC for 100 h. Incipient fusion of salt mixture on the surface of the hot corroded specimen may clearly be seen. These specimens were subjected to high cycle fatigue at 600ºC at different stress amplitudes.

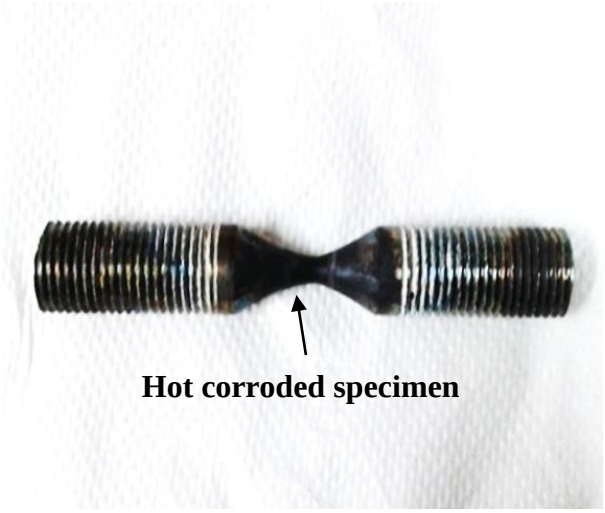

Fig. 5. 1: Digital photographs of the hot corroded HCF specimen.

5.2.2 X-RAY DIFFRACTION ANALYSIS

The nature of the phases formed during the hot corrosion influences the rate of corrosion of the material. The XRD patterns of the Na_2SO_4+NaCl+V_2O_5 (3SM) coated samples, following exposure of 100 h at 600ºC, are shown in Fig. 5.2. The main phases of the hot corroded sample characterized by X-ray diffraction analysis were identified as Ni_3Al, $Ni(VO_3)_2$, Ni_2CrO_4, Ni_3Nb, $CrCl_3$, $FeCl_3$, $NaCrO_2$, $Na_2Cr_2O_7$, Fe_2O_3, Fe_3O_4, $Ni_2V_2O_7$, $FeCr_2O_4$, $NiCr_2O_4$, $NiFe_2O_4$ and $FeVO_4$. The hot corrosion reactions are already shown in Chapter 3.

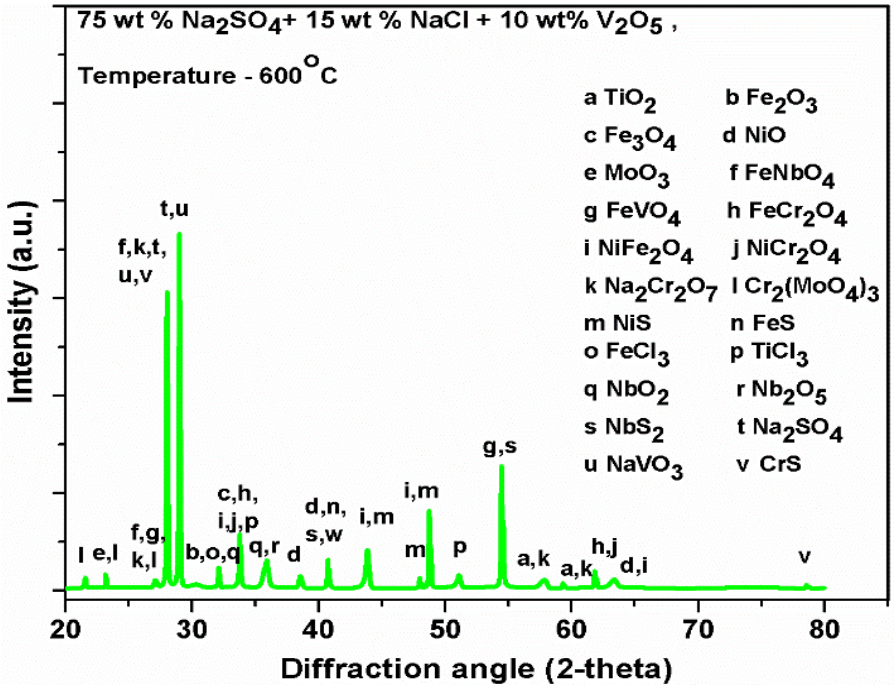

Fig. 5. 2: X-ray diffraction pattern of the sample coated with 75Na_2SO_4 + 15NaCl + 10V_2O_5 (wt.%) salt mixture (3SM) and exposed at 600ºC for 100 h.

5.2.3 FATIGUE LIFE

The dependence of fatigue life (N_f) on stress amplitude at 600ºC at the cyclic frequency of 30 Hz is shown in Fig. 5.3. Decrease in fatigue life was observed with increase in the stress amplitude in both the as heat treated as well as pre hot corroded samples. Drastic reduction in HCF life of the pre hot corroded samples may be attributed to the formation of corrosion pits on the surface.

The data of high cycle fatigue tests for symmetrical cyclic loading are summarized in Tables 5.1 and 5.2. The fatigue limit (σ_e) was found to be 550 MPa for the as heat treated and 450 MPa for the pre hot corroded condition. The coefficient of determination (R^2) of the best fit is 0.95 and 0.99 for the heat treated and pre hot corroded samples respectively in Fig. 5.3 and the horizontal arrow shows the fatigue limit which is based on run-out specimens (not failed up to 10^7 cycles).

Table 5.1: HCF test data of the as heat treated specimens tested at 600ºC, at cyclic frequency of 30 Hz at R= -1.

S No.	Stress amplitude (MPa)	No. of cycles to failure (N_f)
1	450	Not failed, 10^7
2	500	Not failed, 10^7
3	550	Not failed, 10^7
4	600	3.79 X 10^6
5	650	5.73 X 10^5
6	700	3.35 X 10^5
7	750	1.32 X 10^5

Table 5.2: HCF test data of the pre hot corroded specimens tested at 600ºC, at cyclic frequency of 30 Hz at R= -1.

S No.	Stress amplitude (MPa)	No. of cycles to failure (N_f)
1	450	Not failed, 10^7
2	500	2.97 X 10^6
3	550	1.19X 10^6
4	650	7.14X 10^4
5	750	5.10X 10^3

The variation of HCF life with the stress amplitude is analyzed using the Basquin equation **[Campbell (2008)]**: $\sigma_a = \sigma_f' (2N_f)^b$, where σ_a is the stress amplitude, σ_f' is the fatigue strength coefficient, defined as the stress intercept at $2N_f = 1$, $2N_f$ is the number of load reversals to failure, and b is the fatigue strength exponent. The values of σ_f' and b for the as heat treated and pre hot corroded condition are shown in Table 5.3. A lower value of b reflects longer fatigue life.

Table 5.3: High cycle fatigue parameters derived from Basquin relationship.

Condition	Fatigue strength coefficient (σ_f') MPa	Fatigue strength exponent (b)
As heat treated	1698	-0.068
Pre hot corroded	1380	-0.065

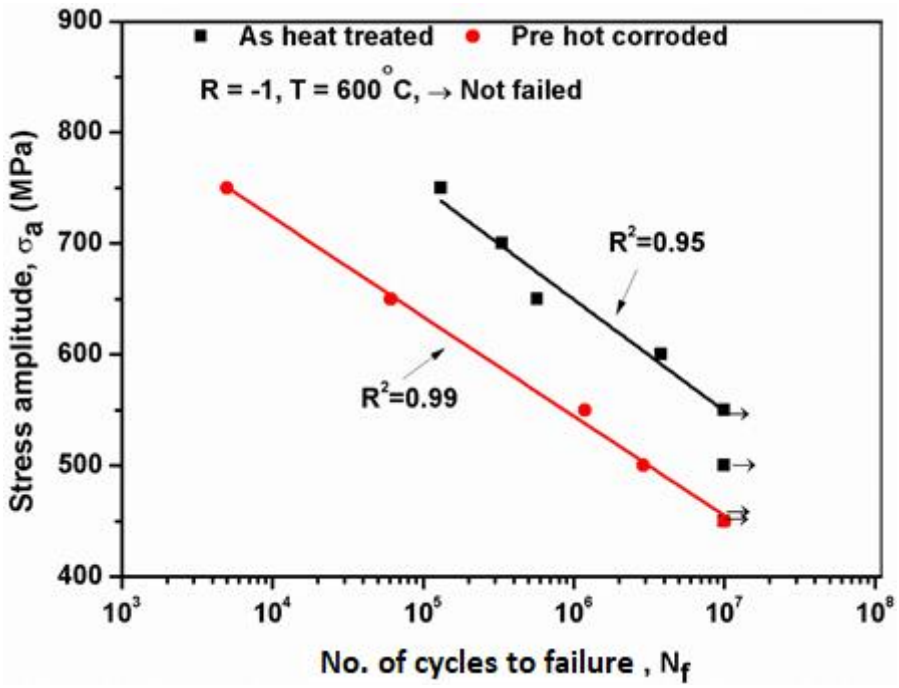

Fig. 5. 3: Variation of fatigue life with stress amplitude at 600ºC, in air, for the as heat treated and pre hot corroded conditions.

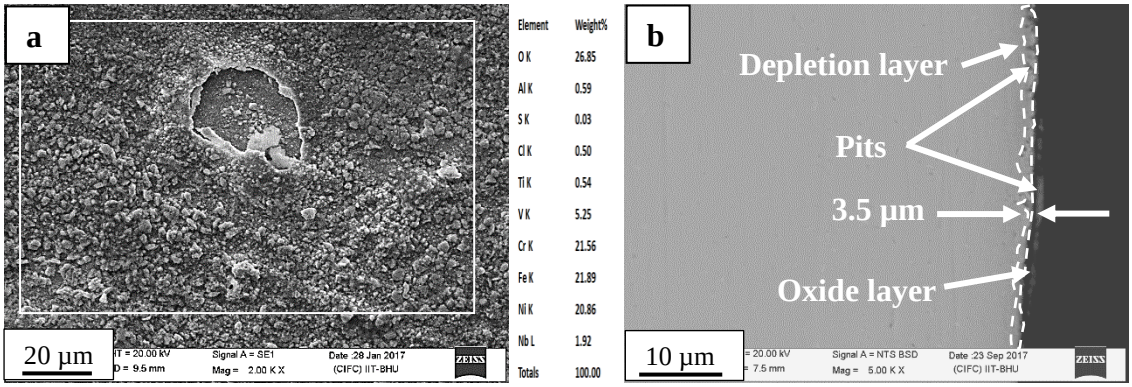

Fig. 5. 4: SEM micrographs of the sample coated with $75Na_2SO_4 + 15NaCl + 10V_2O_5$ (wt.%) salt mixture and exposed at 600ºC for 100 h: (a) surface topography, (b) transverse cross section.

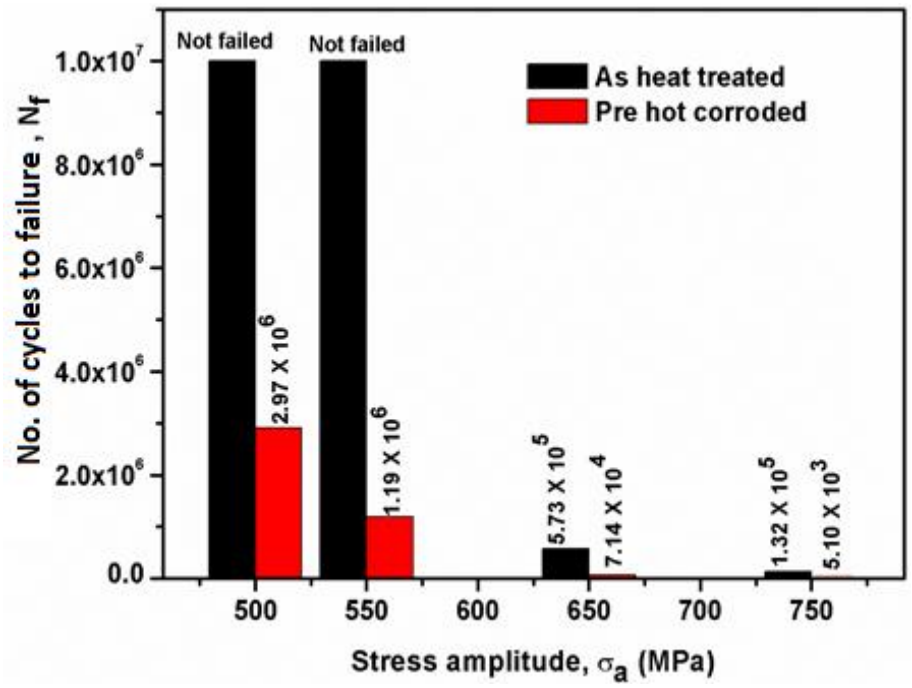

Fig. 5. 5: Histograms showing fatigue life of the as heat treated and pre hot corroded samples, at different stress amplitudes, at 600ºC.

5.2.4 SEM EXAMINATION OF FATIGUE TESTED SPECIMENS

Fracture behavior of the as heat treated and pre hot corroded specimens resulting

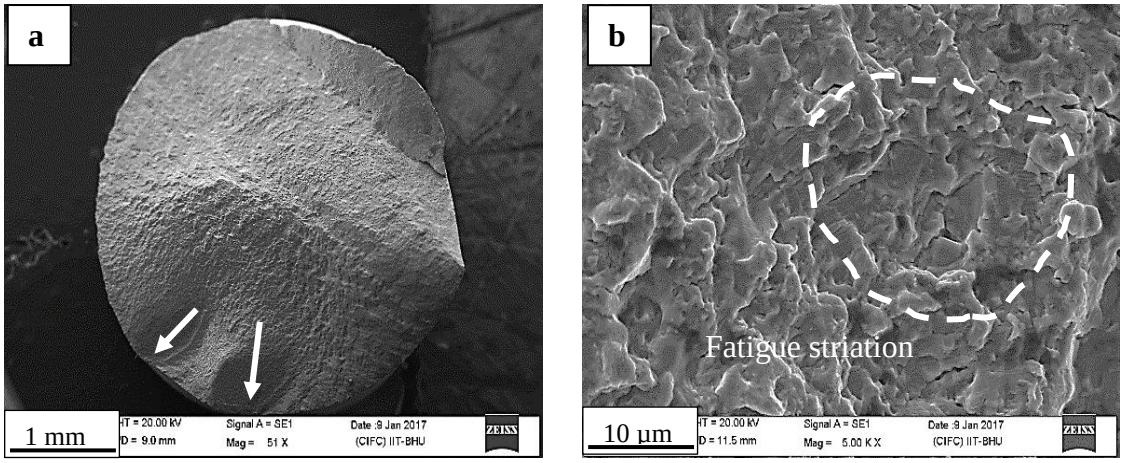

Fig. 5. 6: Fractographs of the as heat treated sample fractured at the stress amplitude of ±650 MPa at 600ºC showing: (a) the fracture surface and crack initiation sites, (b) transgranular crack propagation and extremely fine fatigue striations in the encircled region.

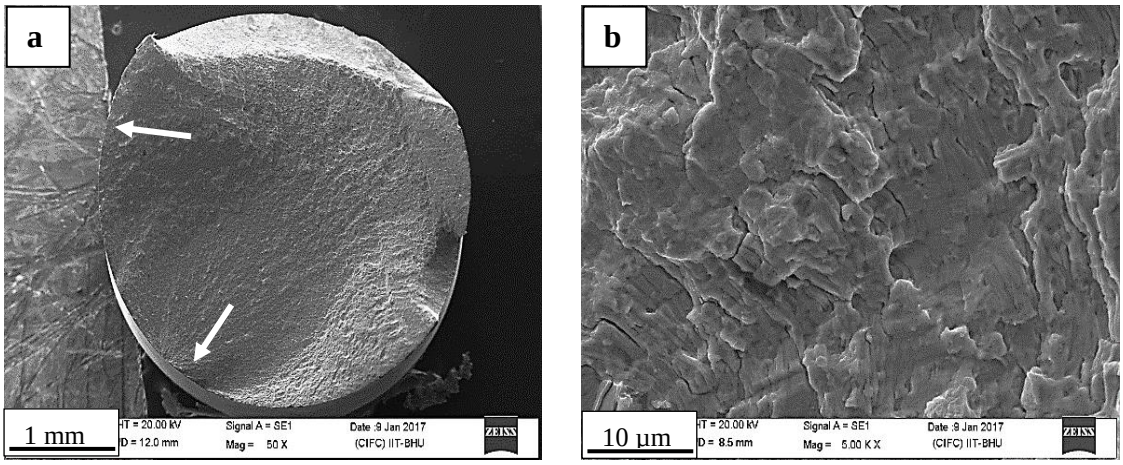

Fig. 5. 7: Fractographs of the as heat treated sample fractured at the stress amplitude of ±750 MPa at 600ºC showing: (a) fracture surface and crack initiation sites, (b) transgranular crack propagation and coarse fatigue striations.

from stress controlled fatigue tests are shown in Figs. 5.6 - 5.13. The larger inter striation spacing on fracture surfaces of the pre hot corroded specimens (Figs. 5.12 (b) and 5.13 (b)) than those on the as heat treated specimens (Figs. 5.6 (b) and 5.7 (b)) may be seen.

Table 5.4: Rate of fatigue crack propagation of the superalloy IN718 in different condition

Stress amplitude (MPa)	**Rate of crack propagation (µm/cycle)**	
	As heat treated	**Pre hot corroded**
500	Not failed	0.38
550	Not failed	0.51
650	0.72	0.92
750	1.21	1.79

Thus, the rate of crack propagation was higher in the pre hot corroded samples. The approximate rates of fatigue crack propagation, evaluated from the fractographs are given in Table 5.4. Fig. 5.14 shows crack population on the curved smooth surface, and the depth of cracks in the longitudinal section of the fatigue fractured specimens is shown in Fig. 5.15.

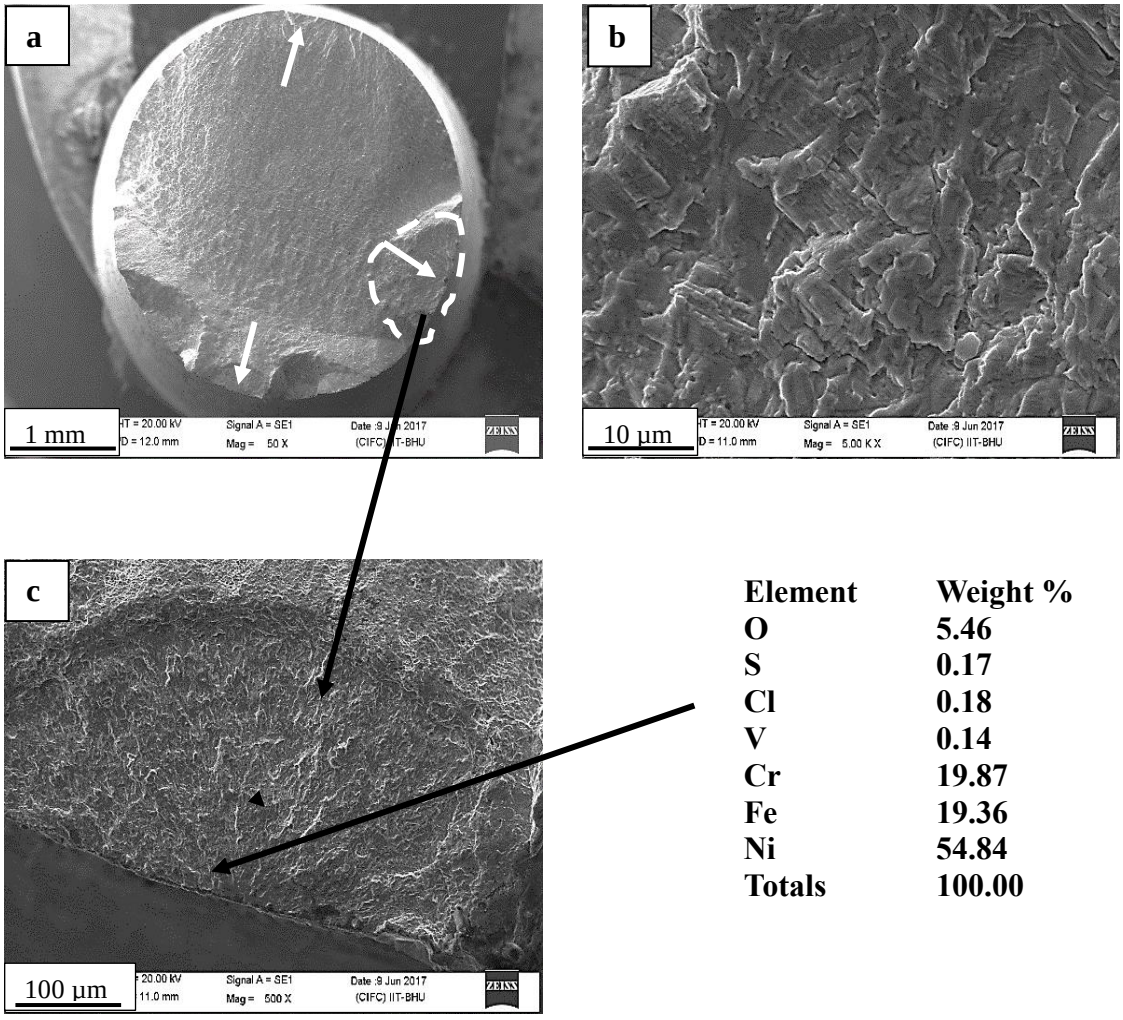

Fig. 5. 8: Fractographs of the fatigue sample pre-corroded and fractured from HCF at the stress amplitude of ±500 MPa at 600ºC in air showing: (a) fracture surface and crack initiation sites, (b) fatigue striations and (c) EDS analysis close to the crack initiation site.

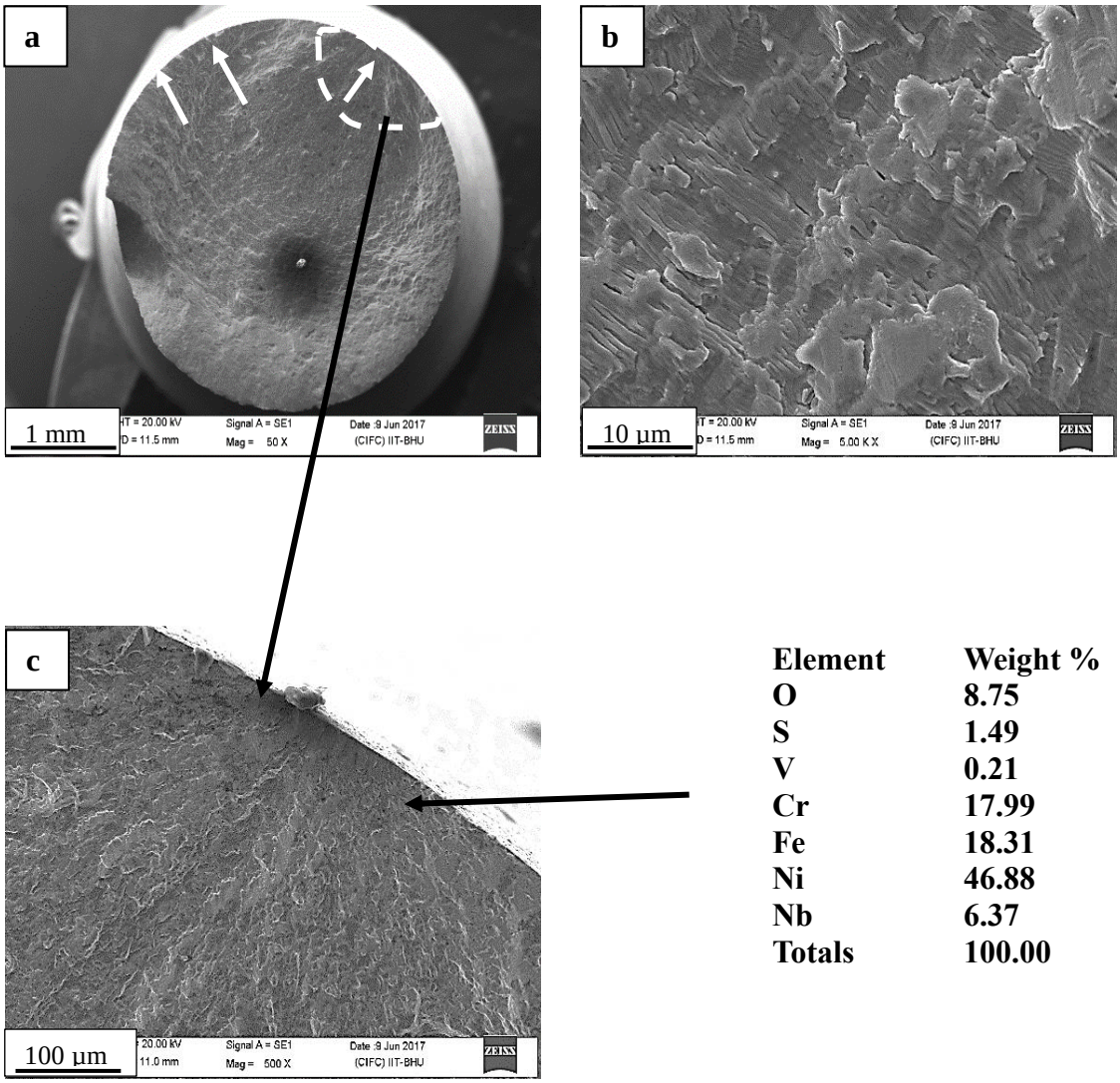

Element	Weight %
O	8.75
S	1.49
V	0.21
Cr	17.99
Fe	18.31
Ni	46.88
Nb	6.37
Totals	100.00

Fig. 5. 9: Fractographs of the fatigue sample pre-corroded and fractured from HCF at the stress amplitude of ±550 MPa at 600ºC in air showing: (a) fracture surface and crack initiation sites, (b) fatigue striations and (c) EDS analysis close to the crack initiation site.

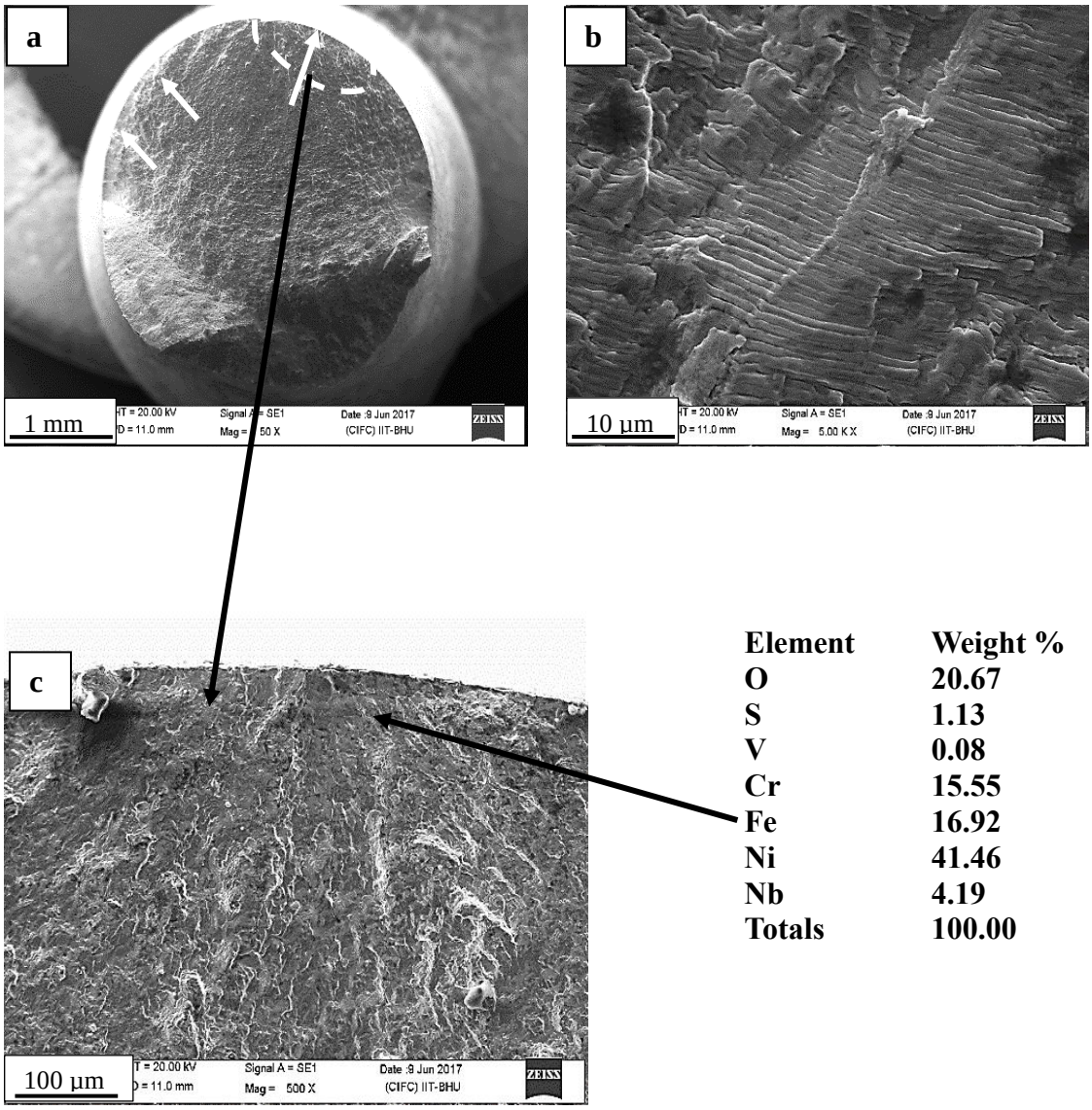

Fig. 5. 10: Fractographs of the fatigue sample pre-corroded and fractured from HCF at the stress amplitude of ±650 MPa at 600ºC in air showing: (a) fracture surface and crack initiation sites, (b) fatigue striations, and (c) EDS analysis close to the crack initiation site.

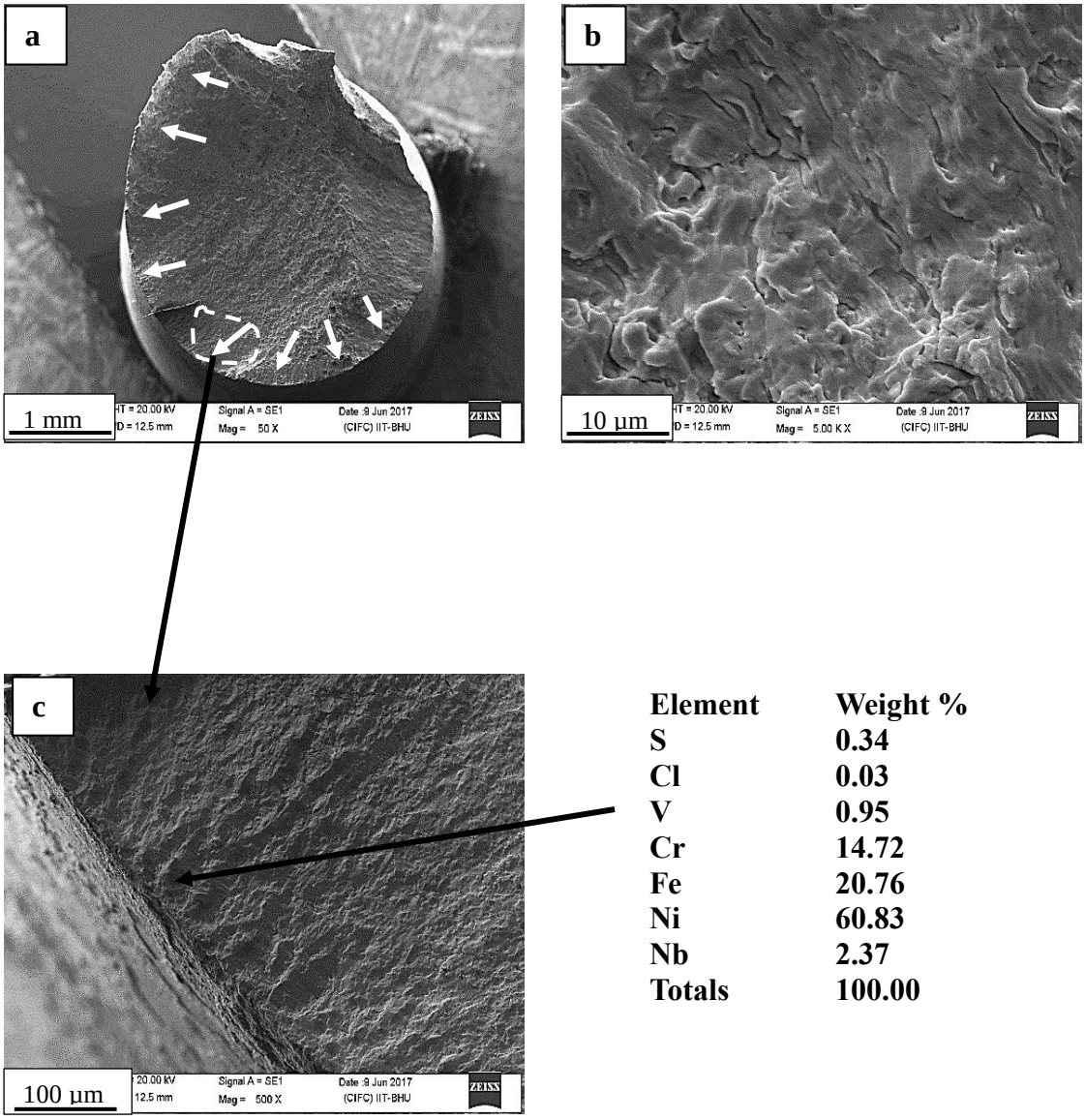

Element	Weight %
S	0.34
Cl	0.03
V	0.95
Cr	14.72
Fe	20.76
Ni	60.83
Nb	2.37
Totals	100.00

Fig. 5. 11: Fractographs of the fatigue sample pre-corroded and fractured from HCF at the stress amplitude of ±750 MPa at 600ºC in air showing: (a) fracture surface and crack initiation sites, (b) fatigue striations, and (c) EDS analysis close to the crack initiation site.

5.3 DISCUSSION

Fig. 5.4 (a) shows surface morphology of the hot corroded sample, coated with the salt mixture of $75Na_2SO_4 + 15NaCl + 10V_2O_5$ (wt.%) (3SM) and exposed at 600ºC for 100 h. The peeled off portion on the surface of the hot corroded sample revealed breakage of the oxide layer by the corrosive species and the traces of corrosive products were confirmed by the EDS analysis. The visual observation showed formation of grayish scale on the hot corroded sample resulting from the incipient fusion of the salt mixture, however, the scale was found to be intact and adherent. Initially a thin layer of oxides of the elements Cr, Fe, Ti, and Nb formed during the first few h, followed by the formation of some chlorides/sulfides which slowly enhanced the process of corrosion in the later stages **[Mannava et al. (2016)]**. In Fig. 5.4 (b) oxide layer and the region of depletion with pits may be seen in the corroded sample. The possible hot corrosion reactions are presented in Chapter 3.

Tables 5.1 and 5.2 present the data of high cycle fatigue tests of the as heat treated and the pre hot corroded samples, tested in the air at 600ºC. Fatigue lives of the pre hot corroded samples are significantly lower than those of the corresponding as heat treated ones. The histograms shown in Fig. 5.5, present fatigue lives of the as heat treated and pre hot corroded samples at different stress amplitudes. As the stress amplitude was increased, there was a drastic reduction in fatigue life of the pre hot corroded samples as compared with that of the as heat treated one. The endurance limit of the pre hot corroded specimens was reduced by 100 MPa in respect of the as heat treated one (Fig. 5.3). The lowering of fatigue strength is attributed to early initiation of fatigue cracks on the surface of the pre hot corroded samples **[Nazmy (1982), Li et al. (2016)]**. The value of fatigue

strength exponent for the as heat treated specimen (b = -0.068) is very close to -0.10 for this alloy, based on the LCF test at 550ºC **[Fournier et al. (1977)]**.

When the samples were subjected to cyclic loading at 30 Hz frequency, there was little spalling of the scale. Figs. 5.8 - 5.11 show SEM fractographs of the pre hot corroded samples in the mixed salt at 600ºC for 100 h and tested in HCF in the air at 600ºC at the stress amplitudes of 500 MPa, 550 MPa, 650 MPa and 750 MPa under symmetric loading (R= -1). Examination of fracture surfaces of the HCF tested samples revealed crack initiation sites along the periphery of the fractured surfaces and transgranular mode of fatigue crack propagation. The regions of fatigue crack growth were evident from the distinct fatigue striations in the as heat treated and pre hot corroded samples (Figs. 5.6 – 5.11). The average inter striation spacing was less in the as heat treated samples as compared with that of the pre hot corroded ones. The pits formed due to hot corrosion and the high stress amplitude escalated the process of fatigue crack initiation and propagation in the pre hot corroded samples due to stress concentration at the pits. The number of crack initiation sites was less (Figs. 8-9) in the as heat treated condition whereas there were multiple crack initiation sites in the pre hot corroded samples (Figs. 5.8 - 5.11).

The EDS analysis shown in Figs. 5.8 (c), 5.9 (c), 5.10 (c) and 5.11 (c) reveals the formation of various deleterious species which penetrated the surface and led to formation of pits, which caused early fatigue crack initiation. It was observed that porous oxide layer provided easy passage to corrosive species like chlorine, sulfur and oxygen into the substrate **[Chapter 3]**. Pits were observed in the cross section wherever metal chlorides evaporated (Fig. 5.4 (b)). Fatigue cracks were initiated from the surface of the both as heat treated as well as pre hot corroded specimens.

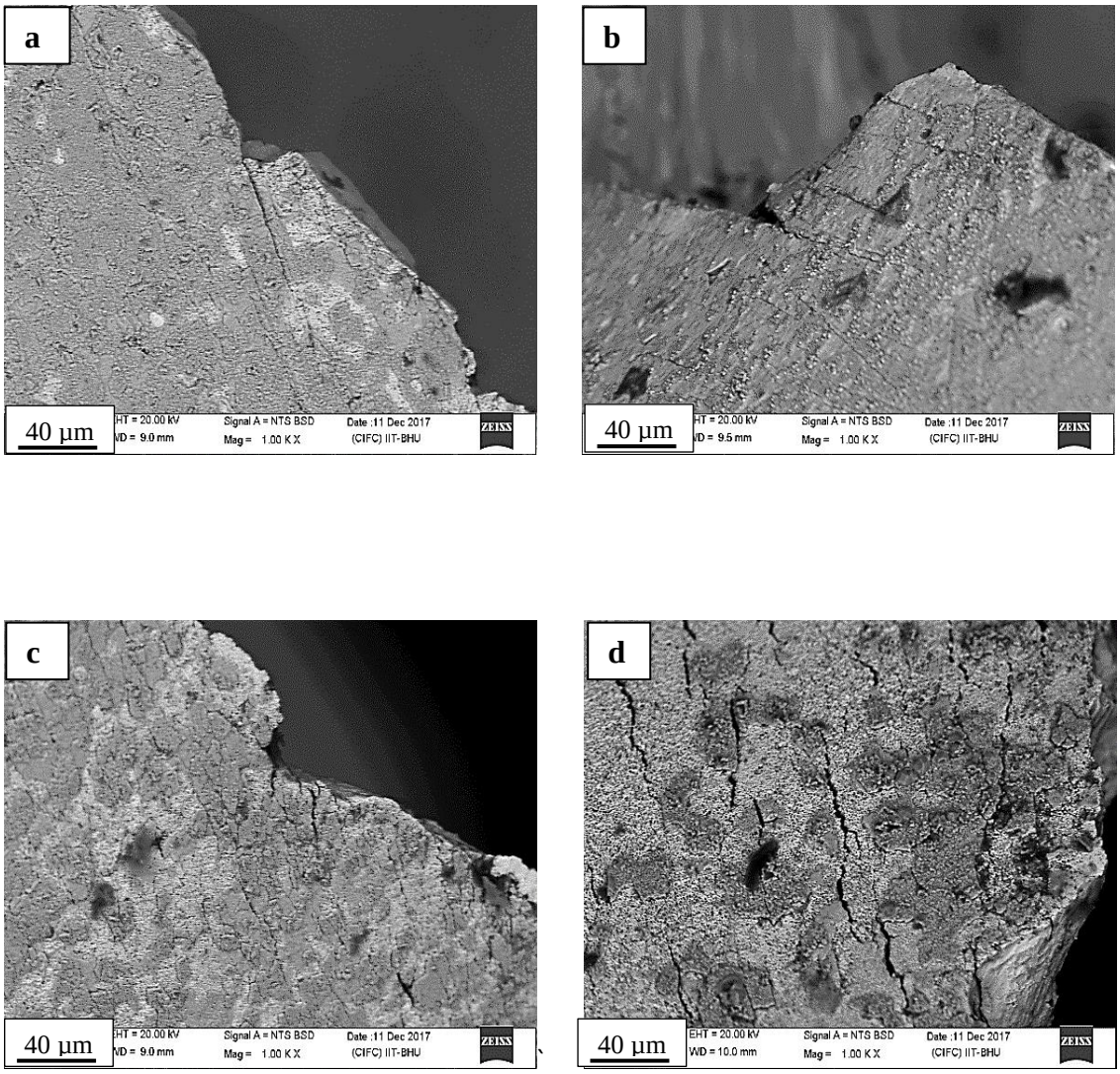

Fig. 5. 12: Backscattered SEM images of curved surfaces of the HCF fractured specimens close to fracture ends, pre corroded in salt mixture with Na_2SO_4 + NaCl + V_2O_5 and tested in HCF at 600ºC at different stress amplitudes: (a) ±500 MPa, (b) ±550 MPa, (c) ±650 MPa and (d) ±750 MPa

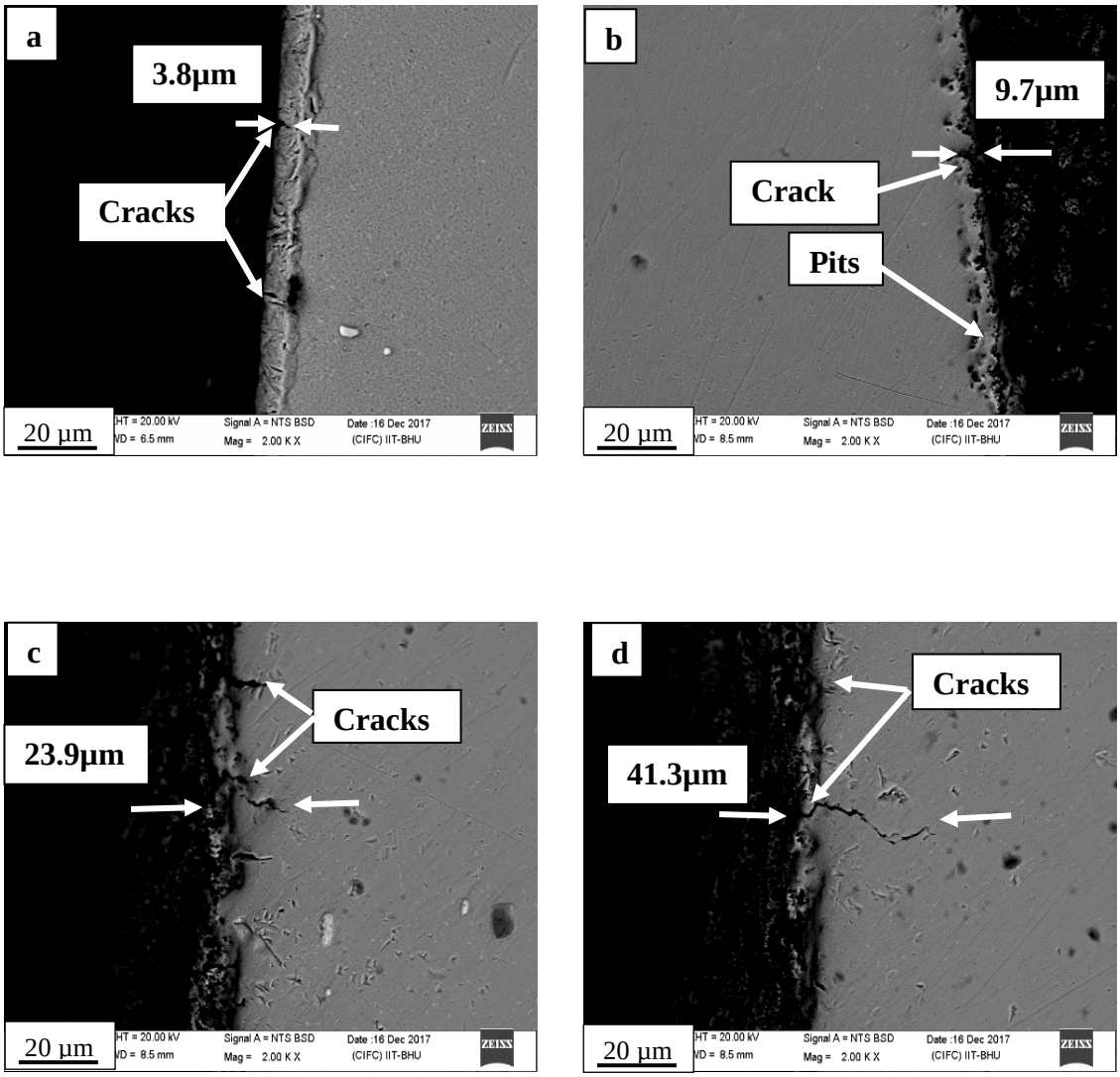

Fig. 5. 13: Backscatter SEM images of longitudinal sections of the specimens pre hot corroded in salt mixture of Na_2SO_4+NaCl+V_2O_5 and HCF tested at different stress amplitudes: (a) ±500 MPa, (b) ±550 MPa, (c) ±650 MPa, and (d) ±750 MPa.

Fig. 5.12 shows crack population on the curved smooth surface, close to the fractured end which clearly shows that the number of cracks increased with increase in the stress amplitude and led to early failure. In the pre hot corroded sample, cracks were initiated from the bottom of the pits due to surface ridging **[Mahobia et al. (2014), Li et al. (2016)]**, which is evident in the longitudinal section of the fatigue fractured specimens (Fig. 5.13). The depth of cracks, close to the fracture end at a comparable distance was found to be 3.8 ± 0.5 µm, 9.7 ± 0.7 µm, 23.9 ± 1.6 µm and 41.3 µm for the samples tested at stress amplitudes of 500 MPa, 550 MPa, 650 MPa and 750 MPa respectively. The pre hot corrosion accelerated the process of damage by fatigue and lowered the fatigue life of the superalloy IN718.

The mechanism of damage from the pre hot corrosion on high cycle fatigue life can be understood from the model proposed in Fig. 5.14. The model is split in two parts: the part I presents the process of hot corrosion and the part II presents the crack initiation and propagation during the high cycle fatigue.

(I) HOT CORROSION MECHANISM

The mechanism of hot corrosion is shown in Fig. 5.14. The salt mixture coated on the surface (Fig. 5.14 a) starts melting on the surface of the specimen. Initially, oxides of Cr, Fe and Ni are formed at the interface of the mixed salt coating and the specimen. Chloride ions break the oxide layer and penetrate into the substrate (Fig. 5.14 b). Formation of metal chlorides was confirmed through XRD analysis (Fig. 5.2). Pitting occurred due to the formation and subsequent evaporation of metal chlorides from the surface. The presence of V_2O_5 increases the oxygen activity and formation of different vandate compounds takes place along with that of $Na_2Cr_2O_7$ (Fig. 5.14 c).

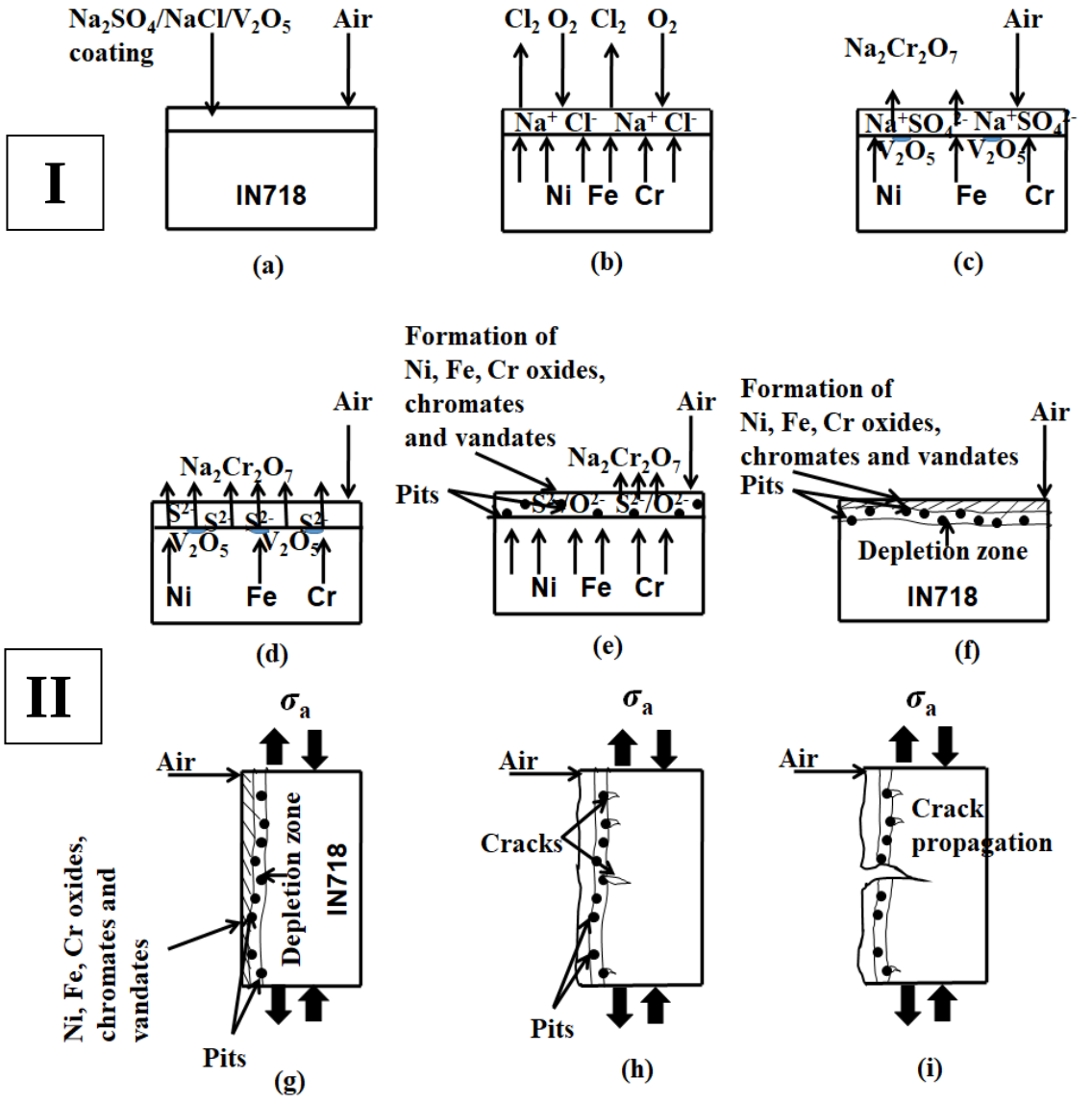

Fig. 5. 14: Mechanism of hot corrosion and crack initiation/growth during the high cycle fatigue: (I) hot corrosion (II) fatigue crack initiation and growth.

Sulfur ions react with Cr, Fe and Ni or their oxides and form their sulfides **[Manaava et al. (2016)]** as shown in Fig. 5.14 (d) and (e). Sulfides are formed from dissociation of nicklates and chromates (Fig. 5.14 f). Thus, Cr gets depleted from the substrate and a depleted region is formed. Hot corrosion of the superalloy IN718 was primarily by oxychlorination process, followed by sulfidation **[Mahobia et al. (2014)]**.

(II) CRACK INITIATION AND PROPAGATION DURING HIGH CYCLE FATIGUE

In the pre hot corroded sample, subjected to cyclic loading at 600ºC in stress controlled mode (Fig. 5.14 g), the early formation of fatigue cracks takes place on the surface from the bottom of the pits (Fig. 5.14 h). The progressive formation of cracks **[Li et al. (2016)]** and their propagation takes place leading to fatigue fracture (Fig. 5.14 i). Thus, fatigue life is reduced due to early fatigue crack initiation and rapid propagation from the pits.

5.4 CONCLUSIONS

Effect of pre hot corrosion of the superalloy IN718 under the coating of salt mixture of $75Na_2SO_4 + 15NaCl + 10\ V_2O_5$ (wt.%) was studied on its high cycle fatigue behavior, at different stress amplitudes under symmetrical loading (R= -1), in air at 600ºC. The following conclusions are drawn:

(a) The hot corroded samples formed grayish and intact scale on the surface of the specimen from the incipient fusion of the salt mixture coating, and the resulting scale was intact and adherent.

(b) Formation of pits from hot corrosion was associated with evaporation of chlorides which provided easy passage for the flow of corrosive constituents in the sample coated with the salt mixture of Na_2SO_4+NaCl+V_2O_5 (3SM).

(c) Lower fatigue resistance of the pre hot corroded samples from the salt mixture of Na_2SO_4+NaCl+V_2O_5 at 600ºC for 100 h, and tested in HCF at 600ºC, was attributed to pit formation and hence early fatigue crack initiation and rapid crack propagation.

(d) The depth of cracks in longitudinal sections of the fractured specimens, close to fracture ends at a comparable distance was found to be 3.8 ± 0.5 µm, 9.7 ± 0.7 µm, 23.9 ± 1.6µm and 41.3 µm for the samples tested at the stress amplitudes of 500 MPa, 550 MPa, 650 MPa and 750 MPa respectively.

(e) The fatigue limit (σ_e) was found to be 550 MPa for the as heat treated specimen and 450 MPa for the pre hot corroded specimen. There was a significant reduction in fatigue life of the pre hot corroded sample over the entire range of the stress amplitudes. The rate of crack propagation was higher in the pre hot corroded samples.